# Stopped-Flow Kinetic Studies of the Interaction between *Escherichia coli* Fpg Protein and DNA Substrates†

Olga S. Fedorova,*,‡ Georgy A. Nevinsky,‡ Vladimir V. Koval,‡ Alexander A. Ishchenko,‡ Nataly L. Vasilenko,‡ and Kenneth T. Douglas*,§

*Novosibirsk Institute of Bioorganic Chemistry, Siberian Division of the Russian Academy of Sciences, Novosibirsk 630090, Russia, and School of Pharmacy and Pharmaceutical Sciences, University of Manchester, Manchester, M13 9PL, U.K.*

*Received July 20, 2001; Revised Manuscript Received November 9, 2001*

ABSTRACT: Formamidopyrimidine−DNA-glycosylase of *Escherichia coli* (Fpg protein) repairs oxidative DNA damage by removing formamidopyrimidine lesions and 8-oxoguanine residues from DNA. This enzyme possesses three types of activities resulting in the excision of oxidized residue from DNA: hydrolysis of the N-glycosidic bond (DNA glycosylase), $\beta$-elimination (AP-lyase), and $\delta$-elimination. In our work, the kinetic mechanism for 8-oxoguanine excision from DNA substrate with Fpg protein has been determined from stopped-flow measurements of changes in the tryptophan fluorescence. The 12-nucleotide duplex d(CTCTC$^{oxo}$GCCTTCC)·d(GGAAGGCGAGAG) containing the 8-oxoG nucleotide in the sixth position of one strand was used as the specific substrate. Four distinct phases in the time traces were detected. These four-phase transition changes in the Fpg protein fluorescence curves were analyzed by global fitting to determine the intrinsic rate constants. We propose that the first two phases represent the equilibrium steps. The first of them describes the bimolecular binding step and the second, formation of the apurinic site. The third, irreversible step is believed to describe the $\beta$-elimination process. The fourth step reflects the $\delta$-elimination and decomposition of complex between enzyme and the product of 8-oxoG nucleotide excision. The results obtained provide direct evidence of conformational transitions of the Fpg protein during the catalytic process. The significance of these results for the functioning of Fpg protein is discussed.

Partial reduction of molecular oxygen can generate reactive oxygen species (ROS),[1] including hydrogen peroxide, and superoxide and hydroxyl free radicals. ROS formation, although a normal cellular activity, is considerably enhanced under chronic inflammatory conditions and ischemia. ROS have been implicated in mutagenesis, carcinogenesis, and aging (*1*−*6*), and are also formed under oxidative stress, UV or ionizing irradiation. Of the cellular macromolecules, DNA is the most susceptible to ROS, which can induce premutagenic modifications of DNA bases, leading to the formation of 8-oxoguanine (8-oxoG), thymine glycols, imidazole ring-opened guanine (2,6-diamino-4-hydroxy-5-formamidopyrimidine, Fapy-G), and imidazole ring-opened adenine (4,6-diamino-5-formamidopyrimidine, Fapy-A). In response, cells have developed elaborate mechanisms to rectify DNA damage, including nucleotide excision and repair. During DNA synthesis in *E. coli*, the appearance of 8-oxoG results in G-C pair replacement by A-T (*2*−*5*). In addition, Fapy blocks the activity of DNA polymerases (*6*), thus causing cell death. Given the vital impact of this lesion, cells have developed a specific repair mechanism. 8-Oxoguanine−DNA-glycosylase (Fpg protein) of *E. coli* removes purine lesions from DNA, including Fapy-G, Fapy-A, and 8-oxoG (*7*). 8-OxoG is believed to be the major physiological substrate for Fpg (*8*). The enzyme has three types of activities: hydrolysis of the N-glycosidic bond and formation of AP-site (DNA-glycosylase), $\beta$-elimination (AP-lyase), and $\delta$-elimination (*7*−*10*). As a result of these functions, the oxidized guanosine residues are excised from the DNA chain. Residue Pro-1 is involved in the glycosylase and AP-lyase activities of the enzyme (*11, 12*). The nitrogen atom of proline attacks at C1′ and, assisted by protonation at O6 of 8-oxoGua, cleaves the glycosidic bond, leading to expulsion of the damaged base. Protonation of the sugar moiety leads subsequently to opening of the deoxyribose ring and Schiff-base formation. The positively charged nitrogen of Pro-1 can facilitate hydrogen abstraction at C2′, and $\beta$-elimination of the C3′ phosphate leads to DNA strand breakage. In the next stage of the catalytic cycle, the complex can undergo $\delta$-elimination of the C5′-phosphate. In the final step, the enzyme is regenerated by attack of the hydroxyl ion on C1′ with release of 4-oxo-2-pentenal (*12*).

† This work was supported by grants from the Wellcome Trust (U.K.), from the Russian Foundation for Basic Research (00-15-97784, 01-04-06268, and 01-04-49003), and from the Siberian Division of the Russian Academy of Sciences.

* To whom correspondence should be addressed. For O.S.F.: phone 7 (3832) 34 42 74, fax 7 (3832) 33 36 77, e-mail fedorova@niboch.nsc.ru. For K.T.D.: phone 44 (0) 161 275 2371, fax 44 (0) 161 275 2481, e-mail Ken.Douglas@man.ac.uk.

‡ Novosibirsk Institute of Bioorganic Chemistry.

§ University of Manchester.

[1] Abbreviations: ROS, reactive oxygen species; Fpg protein, formamidopyrimidine− or 8-oxoguanine−DNA-glycosylase; ODN, oligodeoxyribonucleotide; 8-oxoG, 8-oxoguanosine; Fapy, 2,6-diamino-4-hydroxy-5-formamidopyrimidine and 4,6-diamino-5-formamidopyrimidine; AP, apurinic/apyrimidinic; PAGE, polyacrylamide gel electrophoresis.

10.1021/bi011524u CCC: $22.00 
Published on Web 01/10/2002

Two distinct 8-oxoG-specific glycosylases−$\beta$-lyases (Ogg) have been identified in *Saccharomyces cerevisiae* (*13*−*15*). One of them (Ogg1) recognizes 8-oxoG opposite cytosine, but has little or no effect when the lesion is paired with other DNA bases (*14*, *15*). Recently, a human DNA repair glycosylase, hOGG1, has been cloned (*16*−*18*), and the X-ray structure of its core catalytic domain bound to an oxoG-C-containing duplex oligonucleotide has been reported (*19*).

Recently, we initiated a quantitative study of the molecular principles behind Fpg function (*20*−*23*). The data obtained, combined with structural analysis and thermodynamic characteristics, provide a useful basis from which to elucidate the structure−function properties of the enzyme. Various single-stranded (ss) and double-stranded (ds) ODN substrates (23 bases), containing 8-oxoG in various positions of one strand, were used to define the Fpg protein substrate requirements. Fpg was shown to remove 8-oxoguanine efficiently, not only from double-stranded but also from single-stranded oligodeoxynucleotides. The Michaelis constants ($K_M$) of a range of single-stranded oligodeoxynucleotides (0.55−1.3 $\mu$M) were 12−170 times higher than those for the corresponding double-stranded oligodeoxynucleotides ($K_M$ = 6−60 nM). Depending on the position of the 8-oxoguanine lesion within the oligodeoxynucleotides, relative initial rates of conversion of single-stranded substrates were found to be lower than, comparable to, or higher than those for double-stranded oligodeoxynucleotides.

All these data are consistent with the view that similar interactions occur in the DNA binding cleft of the enzyme for both specific and nonspecific oligodeoxynucleotides. The relative affinities of Fpg protein for specific and nonspecific oligodeoxynucleotides based on $K_i$ values differ by no more than 2 orders of magnitude. Addition of the second complementary chain increases the affinity of the first single-stranded chain by a factor of ~100. Thus, it was concluded that Michaelis complex formation alone of Fpg protein with DNA containing 8-oxoG could not provide the major part of the enzyme specificity, which was found to lie in the $k_{cat}$ term for catalysis, the reaction rate being increased by 6−7 orders of magnitude by the transition from nonspecific to specific oligodeoxynucleotides (*23*).

The interaction of enzyme with nonspecific and specific sites on the substrate, as well as the catalytic process itself, must be accompanied by conformational transitions of the enzyme. In the present study, we have applied stopped-flow fluorescence experiments to reveal individual steps of Fpg−DNA complex formation, to measure the rate constants of steps on the reaction pathway, and to detect transient intermediates. We found that bimolecular encounter of the DNA with the protein is very fast, and accompanied by a fast conformational change, detectable by a change in fluorescence. Subsequent steps, proposed to represent the catalytic stages, were much slower. The apparent rate constants of these steps were fitted to a minimal kinetic model of the reaction pathway.

## MATERIALS AND METHODS

*Fpg Protein*. The enzyme, overexpressed, purified, and stored as described previously (*23*), was electrophoretically homogeneous (specific activity $1 \times 10^5$ units/mg). The Fpg concentration was determined as described (*24*). One unit of enzyme is defined as the amount of enzyme required to catalyze excision of 1 pmol of 8-oxoG from a duplex, d(CTCTCCCTTC $^{oxo}$GCTCCTTTCCTCT)/d(AGAGGAAAG-GAGCGAAGGGAGAG), named in (*22*) as OG11, in 1 min at 25 °C. All experiments were carried out at 25 °C in the following buffer: 50 mM Tris (pH 7.5), 50 mM KCl, 1 mM $Na_2EDTA$, 1 mM DDT, 9% glycerol v/v.

*Enzyme Activity Assay*. The reaction mixture (20 $\mu$L) contained 50 mM Tris-HCl, pH 7.5, 50 mM KCl, 1 mM EDTA, 10 $\mu$g of BSA, 1 mM dithiothreitol, and 9% glycerol; the concentration of ODN(s) was varied. Reactions were initiated by adding Fpg protein and incubated at 25 °C. The reaction products were resolved by electrophoresis in a 20% polyacrylamide gel containing 7 M urea. The $^{32}$P-labeled products were identified by autoradiography. The radioactivities of the bands corresponding to the initial [$^{32}$P]ODNs and various cleavage products were measured by Cherenkov counting (measurements were taken within the linear regions of the time-courses and Fpg concentration curves).

*Synthetic Oligonucleotides*. The 12-mer deoxyribooligonucleotides CTCTC$^{oxo}$GCCTTCC, CTCTCGCCTTCC, and GGAAGGCGAGAG were synthesized using the standard phosphoramidite approach and purified by means of anion-exchange and reversed-phase HPLC. Oligonucleotide concentrations were determined spectrophotometrically at 260 nm with extinction coefficients calculated using pairwise base extinction data (*25*).

*Stopped-Flow Fluorescence Experiments*. A model SX.18MV stopped-flow spectrometer (Applied Photophysics Ltd., Leatherhead, U.K.) fitted with a 150 W Xe arc lamp and 2 mm path length optical cell was used for stopped-flow experiments with excitation at 293 nm. Fluorescence emission from enzyme Trp residues was observed through a 320 nm long-pass filter. The dead time of the instrument was 1 ms. Only data at times >2 ms were used for calculation. Fpg protein in one syringe was rapidly mixed with a solution of substrate in another syringe. The concentration of Fpg protein in all experiments was 1.5 $\mu$M, and concentrations of ODN substrates were varied in the range 0.25−4.0 $\mu$M. Concentrations of reactants reported are those in the reaction chamber after mixing. Typically, each trace shown is the average of four or more individual experiments: reported rate constants represent the mean and standard deviation of such data sets.

*Bleaching of Enzyme Fluorescence*. When a solution of Fpg protein in buffer was mixed with buffer, fluorescence bleaching was observed in this control. For the correction of the measured data, the fluorescence intensities were recalculated using eq 1:

$$F = (F_{obs} - F_b) \times \exp(k_b t) + F_b \quad (1)$$

where $F$ is the corrected fluorescence intensity, $F_{obs}$ is the observed fluorescence intensity, $F_b$ is the background fluorescence, and $k_b$ is the coefficient that was determined for each concentration condition in experiments with nonspecific substrates.

*Inner Filter Effect*. $F$ values in the presence of ODN substrates were also corrected for the inner filter effect due to ODN absorption at 293 nm using the equation:

$$F_c = F \times 10^{0.5A_{ex}} \quad (2)$$

where $F_c$ is the fluorescence intensity at the particular wavelength, corrected both for bleaching and for the inner filter effect, and $A_{ex}$ is the absorbance of the ODNs at 293 nm.

*Kinetic Data Analysis*. The interactions of nonspecific substrates with Fpg protein as well as the first step of the Fpg interaction with specific substrates are described by the equilibrium:

$$E + S \underset{k_{-1}}{\overset{k_1}{\rightleftharpoons}} ES \quad (3)$$

Thus, data were analyzed and fitted using eq 4:

$$[E] = \sqrt{b}\frac{1+c}{1-c} - a \quad (4)$$

where

$$a = \frac{1}{2}\left(s_0 - e_0 + \frac{k_{-1}}{k_1}\right) \quad (5)$$

$$b = a^2 + \frac{k_{-1}}{k_1}e_0 \quad (6)$$

$$c = \frac{e_0 + a + \sqrt{b}}{e_0 + a - \sqrt{b}}\exp(2k_1\sqrt{b}t) \quad (7)$$

The corrected fluorescence intensities, $F_c$, as a function of time at each specific substrate concentration were fit to the sum of four terms:

$$F_c = F1 + F2 + F3 + F4 + C \quad (8)$$

where $C$ is a constant, and

$$F1 = a_1[E]$$

$$F2 = a_2\exp(-k_2^{obs}t)$$

$$F3 = a_3\exp(-k_3^{obs}t)$$

$$F4 = a_4[1 - \exp(-k_4^{obs}t)] \quad (9)$$

where $a_1$, $a_2$, $a_3$, and $a_4$ are the amplitudes and $k_2^{obs}$, $k_3^{obs}$, and $k_4^{obs}$ are the observed rate constants of the second, third, and fourth phases of the observed fluorescence changes, respectively.

*Global Fitting of the Proposed Mechanism to the Stopped-Flow Fluorescence Data*. The global nonlinear least-squares fitting was carried out using the experimental data-fitting package "Scientist" (MicroMath, Inc.) as described (*26*). Differential equations were written for each species in the mechanism in Scheme 1. For global fitting, a set of differential equations was written. The stopped-flow fluorescence traces were directly fit by assigning the corrected fluorescence intensity ($F_c$) as the sum of the background fluorescence ($F$B) and the contribution of each protein species to the total fluorescence intensity at any reaction time $t$, specified by $F0$ through $F3$:

$$F_c = F0 + F1 + F2 + F3 + F\mathrm{B} \quad (10)$$

where $F0 = f_0[E]$, $F1 = f_1[(ES)_1]$, $F_2 = f_2[(ES)_2]$, and $F_3 = f_3[(ES)_3]$; $f_0$ through $f_3$ are the values for specific fluorescence of each Fpg protein species. These specific fluorescence values describe only the part of fluorescence that changes due to DNA binding. [E] through $[(ES)_3]$ are the amounts of each protein species at any given time $t$. Initial values for the intrinsic rate constants $k_1$ through $k_4$ (Scheme 1) were estimated from analysis of the plots of the observed rate constants versus the substrate concentration. First, the set of parameters for the intrinsic rate constants was kept constant, and the specific fluorescence values were floated. Subsequently, one or the other set of parameters was kept constant, and global fitting was used to optimize the floating set. The fitting process was governed by a Marquardt−Levenberg algorithm. The quality of the fit was judged by visual inspection of overlays of the fitted curves and the data as well as inspection of the residuals. Errors in $k_1$ through $k_4$ were around 10%.

*Measurement of Michaelis−Menten Parameters*. The $K_M$ and $V_{max}$ values were estimated using least-squares nonlinear regression analysis and presented using the Cornish−Bowden plot (*27*). Errors in $K_M$ and $V_{max}$ were within 20−50%.

## RESULTS

*Fpg Protein Fluorescence Changes Due to Substrate Binding*. Time-dependent stopped-flow experiments were carried out using the following substrates:

1. specific substrate (oxoG-S):

C−T−C−T−C−$^{oxo}$G−C−C−T−T−C−C
G−A−G−A−G−C−G−G−A−A−G−G

2. nonspecific substrate (NS):

C−T−C−T−C−G−C−C−T−T−C−C
G−A−G−A−G−C−G−G−A−A−G−G

3. specific substrate with AP-site instead of 8-oxoG (AP-S):

C−T−C−T−C−AP−C−C−T−T−C−C
G−A−G−A−G−C−G−G−A−A−G−G

The length of the recognition site of Fpg protein corresponds to 10 nucleotide pairs (*20*−*23*). The lengths of substrate used here were equal to the length of the recognition site with two additional nucleotides to eliminate 5′/3′ end effects.

Fluorescence spectra of Fpg protein in the absence and presence of nonspecific substrate NS were measured under steady-state conditions (Figure 1). On binding to substrates, the spectrum of enzyme was changed, confirming that direct fluorescence monitoring could be used in stopped-flow experiments.

*Kinetics of Fpg Interaction with Nonspecific Substrates.* When Fpg protein was mixed with NS, a decrease in protein fluorescence intensity occurred only in the time range <10 ms (Figure 2). This detected change may reflect the formation of nonspecific encounter complex(es) resulting from random collisions of interacting molecules in solution. The data were fitted using eq 4. This analysis indicated that the formation

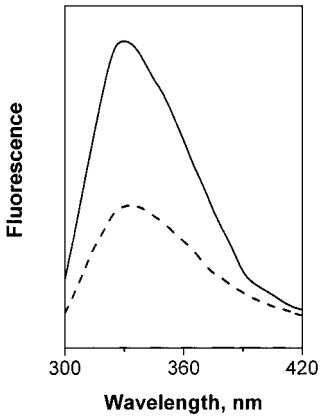


FIGURE 1: Changes in the intrinsic fluorescence spectrum of Fpg protein (free protein, solid line) excited at 293 nm on adding nonspecific oligonucleotide substrate NS (dashed line) ([Fpg] = 1.5 $\mu$M, [NS] = 45 $\mu$M).

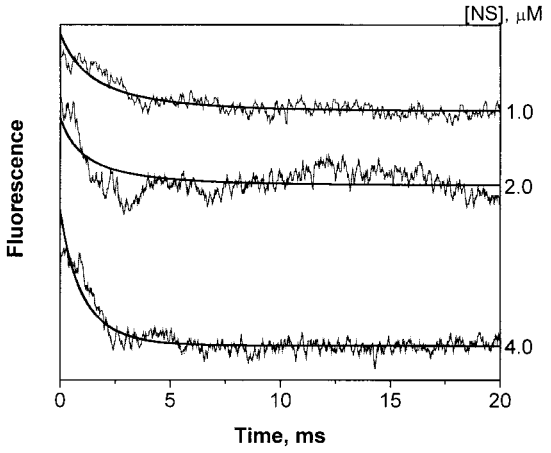


FIGURE 2: Stopped-flow traces (fast stage) of Fpg protein binding at 25 °C with nonspecific substrate NS.

of the first protein−NS complex is encounter-controlled with a forward rate constant of $(2.3 \pm 0.4) \times 10^8$ $M^{-1}$ $s^{-1}$. The reverse rate constant is $(2.7 \pm 0.2) \times 10^3$ $s^{-1}$. Thus, the nonspecific substrate has a weak equilibrium dissociation constant for the complex with Fpg protein, $K_d = 12 \pm 3$ $\mu$M. In a previous study (*23*), we had determined the affinities of different nonspecific ds 8−23-mer oligonucleotides, which were inhibitors of the enzyme, competitive toward substrate. With increase in duplex length, $K_i$ values decreased from 50 to 0.7 $\mu$M; e.g., $K_i$ values were 6.7 and 1.0 $\mu$M for duplexes $d(pA)_{10}$·$d(pT)_{10}$ and $d(pA)_{16}$·$d(pT)_{16}$, respectively.

*A Four-Stage Mechanism for Specific Substrate OxoG-S Interaction with Fpg Protein.* To determine the kinetic mechanism of specific substrate interaction with Fpg protein, stopped-flow experiments were carried out at increasing oxoG-S concentrations. These experiments determined the number of intermediate species in oxoG-S binding and catalytic pathways and the rates of their formation and disappearance. On mixing the samples, several transient changes in the intrinsic Fpg protein fluorescence were observed, and recorded in real time. The protein fluorescence decreased rapidly after mixing with oxoG-S and then more slowly increased (time range 2−100 s). Figure 3 shows representative stopped-flow traces at increasing oxoG-S concentrations (0.25−4.0 $\mu$M).

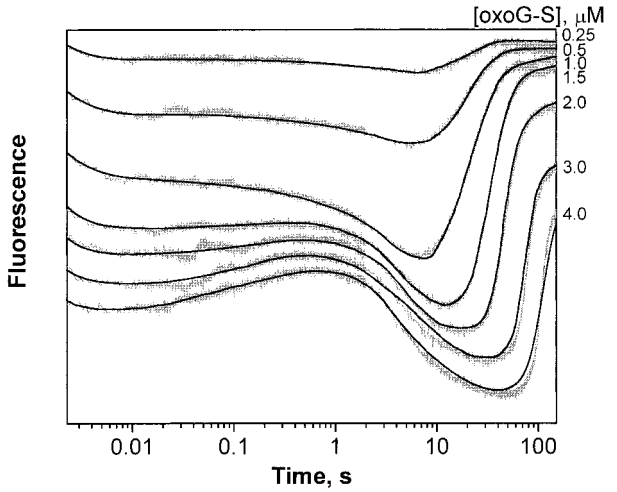


FIGURE 3: Stopped-flow kinetics of oxoG-S interaction with Fpg protein at 25 °C.

Detailed study for the different time ranges indicated the presence of four phases in these traces. The first phase was finished in less than 10 ms. After this, the intensity of fluorescence did not change until around 100 ms. The second phase represents a slow increase in intensity, as is clearly seen at the concentrations 1.5, 2.0, 3.0, and 4.0 $\mu$M. Maxima at around 0.5−1.0 s on these fluorescence traces were detected. The third phase was found at times >1 s, where the fluorescence intensities decreased and minima were observed in the range 10−100 s depending on the initial substrate concentration. After these minima, the fluorescence intensity increased, indicating a fourth phase. If the concentrations of oxoG-S were less than the initial concentration of Fpg protein (single-turnover conditions of enzyme), fluorescence intensities reached the initial values (see curves for [oxoG-S] = 0.25, 0.5, 1.0, and 1.5 $\mu$M). At higher substrate concentrations, the enzyme worked in multiturnover conditions. Therefore, the intensities did not regain their initial values at the observed times, probably due to partial complex formation between Fpg protein and the product of substrate cleavage.

It is clear that the first step is a bimolecular encounter between Fpg protein and specific substrate, oxoG-S. This stage of specific substrate binding was detected separately in the 0−20 ms time range, and analyzed as described above for nonspecific substrate (Figure 4). This analysis indicated that the formation of the first protein·oxoG-S complex is encounter-controlled, with a forward rate constant $k_1$ of $(3.2 \pm 0.3) \times 10^8$ $M^{-1}$ $s^{-1}$. The reverse rate constant $k_{-1}$ is $(8.9 \pm 1.0) \times 10^2$ $s^{-1}$. Thus, the forward rate constant $k_1$ is close to the values obtained for nonspecific substrate NS binding. The reverse rate constant $k_{-1}$ in the case of specific substrate is 3 times lower than for nonspecific substrate.

The second, third, and fourth phases were described by exponential functions as given under Materials and Methods. Exponential rate constants plotted versus the oxoG-S concentration gave the dependencies shown in Figure 5 a−c. The rate constants of the second phase increased in a hyperbolic manner as the oxoG-S concentration was increased and saturated to ~11 $s^{-1}$. The hyperbolic oxoG-S dependence of the second phase provided evidence that the second step contains an equilibrium process. Thus, the bimolecular encounter between Fpg protein and substrate in

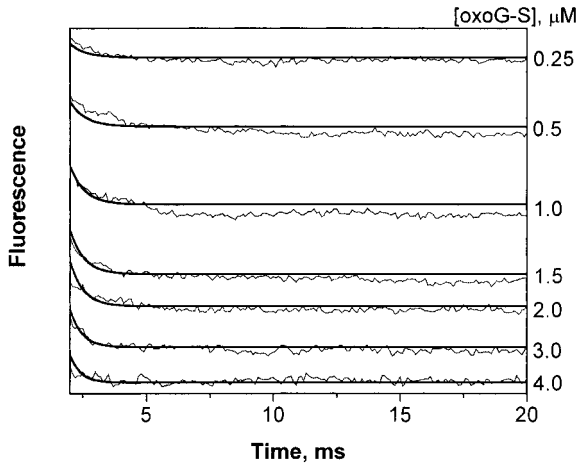


FIGURE 4: Stopped-flow traces (fast stage) of Fpg protein binding at 25 °C with specific substrate oxoG-S.

the first step is followed by a conformational change of protein in the second step. The observed rate constant of the third phase appeared to be independent of oxoG-S concentration, with values close to 0.15 $s^{-1}$. The observed rate constant of the fourth phase varied in the range 0.047−0.105 $s^{-1}$ (see Figure 5c) and decreased with an increase of oxoG-S concentration. The third phase may represent the irreversible step of the catalytic process. In the fourth phase at low oxoG-S concentration (0.25−1.0 $\mu$M), the fluorescence intensity increases to recover its initial value at low concentrations of oxoG-S. This means that free Fpg protein is released. However, at high concentrations of oxoG-S, the final fluorescence intensities are lower than the initial values, an observation that can be explained by complex formation between enzyme and the product of substrate conversion.

Thus, the minimal kinetic scheme describing the observed fluorescence changes may be presented as Scheme 1 where E represents Fpg protein, S is the free oxoG-S, ES1 is the product of the bimolecular encounter, ES2 and ES3 are subsequent states of the Fpg·oxoG-S complex, and P is the product of substrate destruction in the catalytic phase. Constants $k_1$, $k_2$, $k_3$, and $k_4$ characterize the forward direction, whereas $k_{-1}$ and $k_{-2}$ are the rate constants for the reverse reactions.

The intrinsic rate constants of the second, third, and fourth phases could not be determined without solving the explicit equation describing the mechanism. Therefore, the method of numerical integration and global fit of the kinetic data at various DNA concentrations was used to obtain the intrinsic rate constants $k_2$, $k_{-2}$, $k_3$, and $k_4$.

*Global Fit To Obtain the Intrinsic Rate Constants.* The four-stage Fpg−substrate interaction mechanism shown in Scheme 1 was expressed in terms of protein fluorescence changes occurring as a function of time. This procedure, summarized below, is given in more detail under Materials and Methods. In the stopped-flow experiments, the observed fluorescence is the sum of the background fluorescence of the reaction mixture and the fluorescence of each Fpg protein species present at a particular time. The changes in the observed fluorescence occur because part of the protein fluorescence is affected by substrate binding. Therefore, the observed fluorescence throughout a time-course is determined by the accumulation and decay of the different species, which can be described by differential equations. The explicit

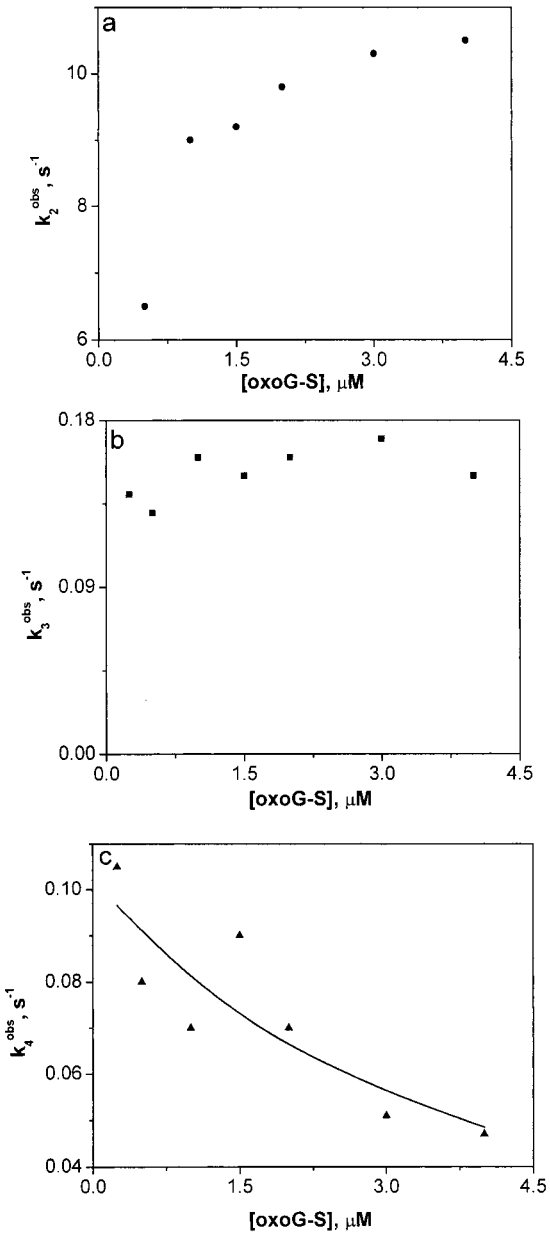


FIGURE 5: Rate constants $k_2^{obs}$ (a), $k_3^{obs}$ (b), and $k_4^{obs}$ (c) as functions of the oxoG-S concentration.

Scheme 1

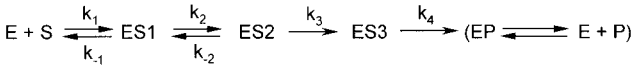


solutions of these equations are possible only in the case where substrate concentration is much higher than enzyme concentration. In this case, the set of linear differential equations can be integrated by standard procedures (*28*, *29*). In our experiments, the concentrations of both interacting molecules were of the same order of magnitude. Therefore, numerical integration of the sum of differential equations was used to fit the stopped-flow kinetic traces and determine the intrinsic rate constants.

The initial conditions were specified according to the reaction conditions. The experimental data for several substrate concentrations were fit simultaneously. To facilitate the fitting process, an iterative approach was chosen in which some of the parameters were fixed and others were opti-

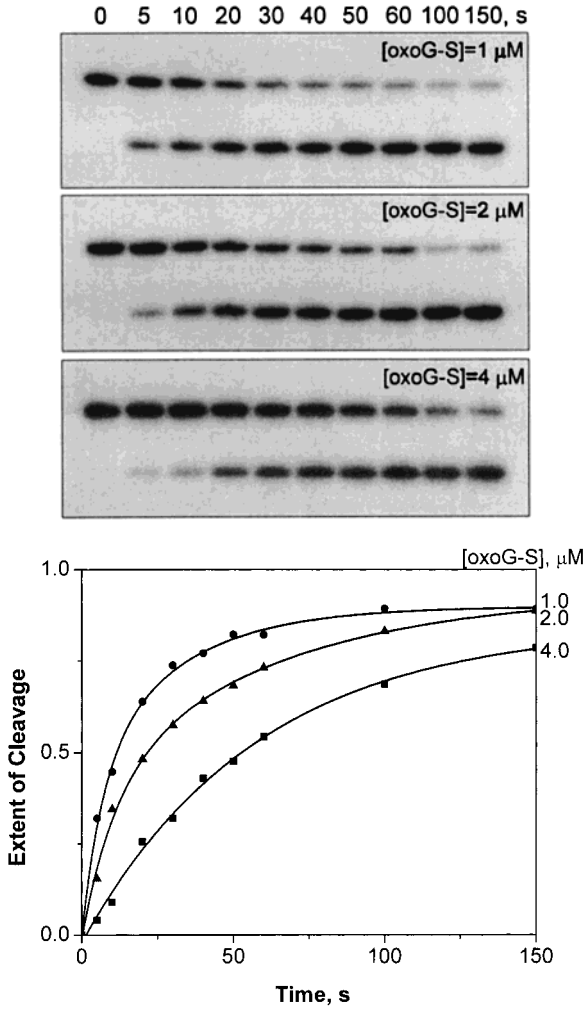


FIGURE 6: Kinetics of substrate oxoG-S cleavage with Fpg protein at 25 °C; PAGE analysis (top panel) and from the extent of cleavage vs time (bottom panel).

mized. Subsequently, the optimized parameters were fixed and the remaining ones were optimized, and so on. Since the rate constants of the first stage ($k_1$, $k_{-1}$) were already determined for the time range 2−20 ms using eq 4, these constants were not estimated during the global fitting procedure. They were fixed, and the rate constants of the second stage ($k_2$, $k_{-2}$) were found for the time range 100 ms−2 s. The rate constants of the third and fourth stages were optimized in the time range 2−100 s with fixed values of $k_1$, $k_{-1}$, $k_2$, and $k_{-2}$. It was apparent that in the third stage the rate constant $k_{-3}$ was not required for the fitting procedure, and the forward reaction rate constant $k_3$ alone was enough to fit the experimental data, in accordance with Scheme 1.

For the fourth stage, the best fitting was achieved by assuming that the apparent rate constant for each curve decreased with an increase in oxoG-S concentration. This phase, characterized with the lowest rate constant, may represent the final catalytic step, in which product is formed. As an external test of this, the rate of product formation in this process was measured directly by PAGE (Figure 6). It can be seen that the dependencies of product yield on time at [oxoG-S] = 1, 2, and 4 $\mu$M correlate well with the rate of increase of fluorescence intensity in the fourth stage. The product of this catalytic process is the duplex in which the 8-oxoG nucleotide is removed from one strand (*12*). The product can be in equilibrium between free and complexed form with the enzyme. Such a complex must decompose in a non-rate-limiting step. The fluorescence traces presented in Figure 3 demonstrate that at low oxoG-S concentrations the initial fluorescence intensities are restored at the end of reaction, in contrast to their decrease in the first phase. It may be concluded that the affinity of the enzyme for such a product is a little lower than for substrate oxoG-S.

Table 1: Rate Constants for Reaction of Fpg Protein at 25 °C with Specific Substrate OxoG-S, Obtained by the Global Fit Procedure

| intrinsic rate constants | global fit |
|---|---|
| $k_1$ ($M^{-1}$ $s^{-1}$) | $(3.2 \pm 0.3) \times 10^{8}$ [a] |
| $k_{-1}$ ($s^{-1}$) | $(8.9 \pm 1.0) \times 10^{2}$ [a] |
| $k_2$ ($s^{-1}$) | $12 \pm 1$ |
| $k_{-2}$ ($s^{-1}$) | $10 \pm 1$ |
| $k_3$ ($s^{-1}$) | $0.16 \pm 0.01$ |
| $k_4$ ($s^{-1}$) | $0.10 \pm 0.01$ |
| $K_{EP}$ ($M^{-1}$) | $(2.8 \pm 0.3) \times 10^{5}$ |

[a] The values $k_1$ and $k_{-1}$ were determined separately according to equilibrium 3 and eq 4.

The fitting procedure assumed that the apparent rate constant of the fourth stage decreased with increase in oxoG-S concentration due to equilibrium complex formation between enzyme and the product:

$$E + P \rightleftarrows EP\ (K_{EP}) \qquad (11)$$

Therefore, the intrinsic rate constant of the fourth phase, denoted as $k^*_4$, depends on concentration of product P and the equilibrium stability constant $K_{EP}$ according to eq 12:

$$k^*_4 = \frac{k_4}{1 + K_{EP}[P]} \qquad (12)$$

where [P] is the concentration of product P in solution. Equation 12 was taken into account in the description of fluorescence traces with the set of differential equations. Thus, a single set of rate constants, equilibrium association constant $K_{EP}$, and fluorescence factors was obtained that best described the experimental data. The values of the rate constants and the equilibrium association constant $K_{EP}$ are presented in Table 1. It can be seen from Table 1 that the values of the rate constants $k_2$, $k_3$, and $k_4$ do not differ significantly from the corresponding values obtained in the preliminary kinetic analysis. The intrinsic rate constants $k_1$ through $k_4$ and fluorescence factors were used to simulate the stopped-flow kinetics and gave good agreement with observed stopped-flow data (solid curves in Figure 3).

*Determination of $K_M$ and $k_{cat}$ Values*. To analyze how the obtained rate constants agree with the Michaelis−Menten parameters, $K_M$ and $k_{cat}$, these were estimated for oxoG-S and AP-S. These values were found to be the following: $K_M = 2.0 \pm 1.0$ $\mu$M and $k_{cat} = (2.5 \pm 1.0) \times 10^{-2}$ $s^{-1}$ for oxoG-S substrate; $K_M = 4.6 \pm 1.0$ $\mu$M and $k_{cat} = (5.0 \pm 1.5) \times 10^{-2}$ $s^{-1}$ for AP-S (these values were determined by PAGE; see Figure 6). The value of $k_4$ was found to be 0.1 $s^{-1}$ by stopped-flow studies for the specific substrate oxoG-S (Table 1). As the $k_{cat}$ value is estimated from PAGE experiments, the precision is much less than that associated with the determination of $k_4$. The difference of 4-fold could easily arise from the difference in techniques. It is not

Scheme 2

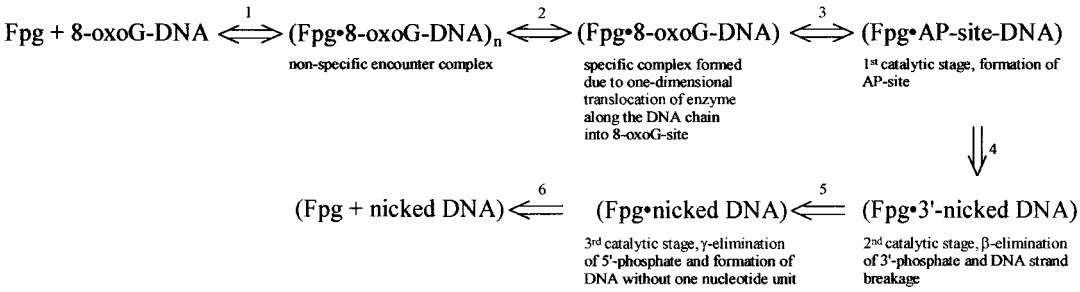


justified to analyze the 4-fold difference as indicating that the $k_{cat}$ term does not refer to a particular rate step but is a kinetic constant with contributions from some other steps as well as $k_4$. It is most likely that $k_{cat}$ does indeed largely reflect the same process as $k_4$.

## DISCUSSION

The results reported here directly establish the minimal mechanism of interaction of 8-oxoguanine-containing 12-mer duplex (oxoG-S) with the Fpg repair enzyme. The kinetic pathway of oxoG-S interaction was determined by following the transient changes in the intrinsic Fpg protein fluorescence using stopped-flow methods. As Fpg protein has five tryptophan residues, protein tryptophan fluorescence was monitored under excitation at 293 nm. The observed fluorescence changes could result from global conformational changes in the protein upon substrate binding and catalysis stages. Stopped-flow traces indicate the existence of at least three conformational transitions in Fpg substrate-processing.

According to recent views and our previous data, enzymes acting on lengthy DNA are capable of binding to DNA of any sequence in the first stage, and then "sliding" along to a site containing a specific nucleotide unit or sequence [reviewed in Bugreev and Nevinsky (*30*)]. On locating this site, they focus here due to their greater affinity for it. Since intercalation of the side chains of hydrophobic amino acid residues of enzymes (a rather frequent phenomenon) between the DNA bases in specific sequences is favored in comparison with other DNA sites, an effective partial or complete melting of this zone of DNA occurs. X-ray analysis data for the core of hOGG1 (*19*), which like Fpg protein can excise 8-oxoG and structurally related lesions (glycosylase activity) and cleave the DNA backbone ($\beta$-lyase activity) (*15*, *16*, *18*, *31*), show that hOGG1 wedges the aryl ring of Tyr 203 between the bases, thereby unstacking the bases and creating a sharp kink in the DNA. After this point, additional changes in the DNA structure, including its partial melting, occur, to stabilize a highly unusual DNA backbone conformation at the site of lesion as the enzyme tries to swivel the 8-oxoG residue out of the helix using the bent and kinked conformation (*19*). Formation of many additional bonds between hOGG1 and structural elements of DNA and its 8-oxoG base promotes the proper "folding" of specific bases into "pockets" of the enzyme, with acceleration of the reaction. Since hOGG1 and Fpg protein are very similar enzymes, similar changes of DNA structure are likely to occur for Fpg protein.

In contrast to hOGG1, Fpg protein catalyzes not only $\beta$-elimination (AP-lyase) but also an $\delta$-elimination. There are no available data on whether the glycosylase and AP-lyase active centers of Fpg protein are coincident. If they are noncoincident, after removing the 8-oxoG base the apurinized DNA has to translocate to the enzyme AP-lyase center. Alternatively, there may be reorganization of the DNA−enzyme complex if these centers are combined on the enzyme. Obviously, interaction of Fpg protein with specific DNA proceeds in many steps. Taking all the above data into account, interaction of Fpg protein with specific DNA containing 8-oxoG can be described in principle using Scheme 2, where (Fpg•8-oxoG-DNA)$_n$ is the nonspecific encounter complex, (Fpg•8-oxoG-DNA) is the specific complex formed as a result of one-dimensional enzyme translocation along the DNA chain, (Fpg•AP-site-DNA) is the complex with apurinic DNA substrate formed in the first catalytic stage, (Fpg•3′-nicked AP-site-DNA) is the complex with DNA substrate, where the strand is nicked in the second catalytic stage as the result of $\beta$-elimination of the 3′-phosphate end, and (Fpg•nicked DNA) is the complex formed in the third catalytic stage as the result of $\delta$-elimination of the 5′-phosphate end and formation of DNA substrate without one nucleotide unit.

Thus, there are at least six stages in the repair process at which enzyme conformational transitions could occur. The first three stages represent equilibrium processes, including the third stage where the intermediate with an AP-site is formed (*32*−*34*). Our experimental data are consistent with a minimal model containing four steps and three conformational transitions. The first phase is characterized by the largest change of fluorescence intensity of the protein. The forward rate constant $k_1 = (3.2 \pm 0.3) \times 10^8$ M$^{-1}$ s$^{-1}$ of this phase corresponds to an encounter-controlled reaction and has approximately the same values for nonspecific and specific substrates. This means that this phase is the formation of encounter complex(es) resulting from occasional random collision of interacting molecules in solution. The reverse process is very fast, with rate constant $k_{-1}$ equal to $(8.9 \pm 1.0) \times 10^2$ s$^{-1}$ for the specific substrate and $(2.7 \pm 0.2) \times 10^3$ s$^{-1}$ for the nonspecific substrate. Due to the short length of the nucleotide chain in oxoG-S and NS, we would not see the sliding process of the enzyme moving along the chain even if, in principle, this sliding could take place. Therefore, in the case of both substrates, complex ES1 represents the complex (Fpg•8-oxoG-DNA). Like many other DNA-dependent enzymes, Fpg protein, in principle, can form complexes with any nonspecific DNA. According to previous results (*20*−*22*), such complexes exist due to multiple, weak, nonspecific additive contacts between Fpg protein and the DNA backbone.

In the case of the specific oxoG-S substrate, the first enzyme−substrate complex, ES1, resulting from the bimolecular encounter, is transient and converts to ES2 at a forward rate constant $k_2$ of 12 ± 1 $s^{-1}$, with a reverse rate constant $k_{-2}$ of 10 ± 1 $s^{-1}$. The ES2 intermediate subsequently converts to ES3 with rate constant $k_3 = 0.16 \pm 0.01$ $s^{-1}$. The rate constant of the reverse step, $k_{-3}$, was not identified, and the conversion of ES2 into ES3 is probably an effectively irreversible step.

The fourth phase is characterized by rate constant $k_4$ that decreased with increase of substrate oxoG-S concentration. In this step, the fluorescence regains its initial value only at low oxoG-S concentration. This is reasonable and suggests that the product formed as a result of removal of damaged nucleoside has lower affinity than substrate for Fpg protein.

The equilibrium constants for each step in Scheme 1 are $K_1 = k_1/k_{-1}$ and $K_2 = k_2/k_{-2}$. Introducing the values of the rate constants gives $K_1 = (3.6 \pm 0.4) \times 10^5$ $M^{-1}$ and $K_2 = 1.2 \pm 0.2$. The overall binding constant $K_b$ is related to the partial equilibrium steps by

$$K_b = K_1(1 + K_2) \quad (13)$$

Introducing the values of equilibrium constants for partial equilibrium steps into eq 13 gives $K_b = (7.9 \pm 1.5) \times 10^5$ $M^{-1}$. Therefore, the $K_d$ value for this enzyme−substrate complex is equal to 1.3 ± 0.4 $\mu$M. This $K_d$ value is comparable to the standard Michaelis constant $K_M$ calculated using Cornish−Bowden plots: $K_M = 2.0 \pm 1.0$ $\mu$M for oxoG-S substrate and $K_M = 4.6 \pm 1.0$ $\mu$M for the apurinic substrate, AP-S. It was shown in a previous study (*22*) that $K_M$ values for this enzyme are around 10 nM for the 23-mer duplex OG11, d(CTCTCCCTTC$^{oxo}$GCTCCTTTCCTCT)·d(AGAGGAAAGGAGCGAAGGGAGAG), containing the 8-oxoG residue in the 11th position of one strand. However, shortening the duplex to a 12-mer led to an increase in $K_M$.

An important question to consider concerns the nature of intermediates ES2 and ES3. As mentioned above, Fpg protein catalyzes hydrolysis of a DNA substrate at two stages. First, modified 8-oxoG is removed from DNA. In the next stage, Fpg protein catalyzes the two-step removal of the sugar moiety from the AP-site of DNA via formation of an intermediate, a Schiff-base between the enzyme and the aldehyde group of the apurinic site in DNA (*11*, *12*).

According to the X-ray analysis data (*19*) for the hOGG1 enzyme, removal of the 8-oxoG residue proceeds due to significant changes of structure of both enzyme and DNA. Phosphate backbone interactions with hOGG1 should provide stabilization of a highly unusual DNA backbone conformation at the site of lesion since the enzyme tries to swivel the 8-oxoG residue out of the helix using the bent and kinked conformation of DNA. The 8-oxoG residue can form several different contacts with amino acid residues of the lesion pocket only after significant change(s) in DNA conformation. Thus, it is reasonable to suggest that this stage of the adaptation of DNA to its optimal conformation for catalysis should be relatively slow. The same situation has to be achieved in the case of Fpg protein.

The following reorganization of the Fpg protein complex with DNA, leading to the formation of a Schiff-base intermediate with the Pro-1 residue of the enzyme, as well as elimination of the sugar moiety, should also be relatively slow. It should be noted that it is precisely these two steps of the catalytic process, which may be accompanied by a major change of the enzyme structure, as in the case of hOGG1 enzyme (*19*). As a consequence, it is reasonable to envisage these steps of the reaction as being accompanied by a noticeable change in protein fluorescence. Thus, it is natural to assign ES2 and ES3 to Fpg-dependent steps of removal of base and sugar moieties of DNA, respectively. ES2 is the complex of Fpg protein with apurinized substrate (Fpg·AP-site-DNA). In this complex, $\beta$-elimination takes place, resulting in the cleavage of the DNA chain. Therefore, this step must be irreversible and leads to formation of intermediate ES3 representing the Schiff-base between Pro-1 and the aldehyde group of the apurinic site in a cleaved substrate, namely, (Fpg·3′-nicked AP-site-DNA).

The complex ES3 completes the sequence of catalytic steps. This complex must first be converted to a complex of enzyme with the product of substrate transformation EP, where P is the nicked DNA (one nucleotide is removed from one DNA strand), as in Scheme 2. It is reasonable to suggest that the decomposition of this complex to free E and P molecules must be a non-rate-limiting step, because the affinity of the Fpg protein for the product must be not higher than for specific substrate. Therefore, the fourth phase on the fluorescence traces represents two steps of the enzyme process: $\delta$-elimination of the 5′-phosphate (i.e., the formation of DNA without one nucleotide unit in one strand), and decomposition of the complex between Fpg protein and nicked DNA. The complex EP has a little lower stability, as does complex ES1.

The values of $k_{cat}$, estimated from the Cornish−Bowden plot for substrates oxoG-S and AP-S, do not differ significantly from the $k_4$ value. Thus, the fourth stage is rate-limiting in this catalytic process.

In summary, the stopped-flow analysis of the interaction of Fpg protein with specific and nonspecific substrates has permitted the determination of the intrinsic rate constants of this multistep enzyme process. This provides a minimal kinetic model for the reaction sequence on a quantitative basis.

## ACKNOWLEDGMENT

We thank Dr. Dmitri V. Pyshnyi for technical assistance and A. V. Charkova for help in the preparation of figures.

## REFERENCES

1. Cathcart, R., Schwiers, E., Saul, R. L., and Ames B. N. (1984) *Proc. Natl. Acad. Sci. U.S.A. 81*, 5633−5637.
2. Richter, C., Park, J. W., and Ames B. N. (1988) *Proc. Natl. Acad. Sci. U.S.A. 85*, 6465−6467.
3. Adelman, R., Saul, R. L., and Ames B. N. (1988) *Proc. Natl. Acad. Sci. U.S.A. 85*, 2706−2708.
4. Cutler, R. G. (1991) *Am. J. Clin. Nutr. 53*, 373S−379S.
5. Ames, B. N. (1983) *Science 221*, 1256−1264.
6. Ames, B. N. (1989) *Free Radical Res. Commun. 7*, 121−128.
7. Boiteux, S., Gajewski, E., Laval, J., and Dizdaroglu, M. (1992) *Biochemistry 31*, 106−110.
8. Tchou, J., Kasai, H., Shibutani, S., Chung, M. H., Laval, J., Grollman, A. P., and Nishimura, S. (1991) *Proc. Natl. Acad. Sci. U.S.A. 88*, 4690−4694.
9. Tchou, J., Bodepudi, V., Shibutani, S., Antoshechkin, I., Miller, J., Grollman, A. P., and Johnson, F. (1994) *J. Biol. Chem. 269*, 15318−15324.

10. Karakaya, A., Jaruga, P., Bohr, V. A., Grollman, A. P., and Dizdaroglu, M. (1997) *Nucleic Acids. Res. 25*, 474−479.
11. Tchou, J., and Grollman, A. P. (1995) *J. Biol. Chem. 270*, 11671−11677.
12. Zharkov, D. O., Rieger, R. A., Iden, C. R. and Grollman, A. P. (1997) *J. Biol. Chem. 272*, 5335−5341.
13. De Oliveira, R., Van Der Kemp, P. A., Thomas, D., Geiger, A., Nehls, P., and Boiteux, S. (1994) *Nucleic Acids Res. 22*, 1760−1764.
14. Van Der Kemp, P. A., Thomas, D., Barbey, R., de Oliveira, R., and Boiteux, S. (1996) *Proc. Natl. Acad. Sci. U.S.A. 93*, 5197−5202.
15. Nash, H. M., Bruner, S. D., Scharer, O. D., Kawate, T., Addona, T. A., Spooner, E., Lane, W. S., and Verdine, G. L. (1996) *Curr. Biol. 6*, 968−980.
16. Radicella, J. P., Dherin, C., Desmaze, C., Fox, M. S., and Boiteux, S. (1997) *Proc. Natl. Acad. Sci. U.S.A. 94*, 8010−8015.
17. Arai, K., Morishita, K., Shinmura, K., Kohno, T., Kim, S. R., Nohmi, T., Taniwaki, M., Ohwada, S., and Yokota, J. (1997) *Oncogene 14*, 2857−2861.
18. Roldan-Arjona, T., Wei, Y. F., Carter, K. C., Klungland, A., Anselmino, C., Wang, R. P., Augustus, M., and Lindahl, T. (1997) *Proc. Natl. Acad. Sci. U.S.A. 94*, 8016−8020.
19. Bruner, S. D., Norman, D. P. G., and Verdine, G. L. (2000) *Nature 403*, 859−865.
20. Ishchenko, A. A., Bulychev, N. V., Maksakova, G. A., Johnson, F., and Nevinskii, G. A. (1998) *Mol. Biol. (Moscow) 32*, 549−558.
21. Ishchenko, A. A., Bulychev, N. V., Maksakova, G. A., Johnson, F., and Nevinsky, G. A. (1999) *IUBMB Life 48*, 613−618.
22. Ishchenko, A. A., Koval, V. V., Fedorova, O. S., Douglas, K. T., and Nevinsky, G. A. (1999) *J. Biomol. Struct. Dyn. 17*, 301−310.
23. Ishchenko, A. A., Bulychev, N. V., Maksakova, G. A., Johnson, F., and Nevinsky, G. A. (1997) *Biochemistry (Moscow) 62*, 204−211.
24. Smith, P. K., Krohn, R. I., Hermanson, G. T., Mallia, A. K., Gartner, F. H., Provenzano, M. D., Fujimoto, E. K., Goeke, N. M., Olson, B. J., and Klenk, D. C. (1985) *Anal. Biochem. 150*, 76−85.
25. Fasman, G. D., Ed. (1975) *Handbook of Biochemistry and Molecular Biology*, 3rd ed., Vol. II, p 589, CRC Press, Cleveland, OH.
26. Picha, K. M., Ahnert, P., and Patel, S. S. (2000) *Biochemistry 39*, 6401−6409.
27. Cornish-Bowden, A. (1976) *Principles of Enzyme Kinetics*, pp 160−206, Butterworths, London.
28. Bujalowski, W., and Jezewska, M. J. (2000) *Biochemistry 39*, 2106−2122.
29. Bujalowski, W., and Jezewska, M. J. (2000) *J. Mol. Biol. 295*, 831−852.
30. Bugreev, D. V., and Nevinsky, G. A. (1999) *Biochemistry (Moscow) 64*, 237−249.
31. Shinmura, K., Kasai, H., Sasaki, A., Sugimura, H., and Yokota, J. (1997) *Mutat. Res. 385*, 75−82.
32. Dodson, M. L., Michaels, M. L., and Lloyd, R. S. (1994) *J. Biol. Chem. 269*, 32709−32712.
33. Sun, B., Latham, K. A., Dodson, M. L., and Lloyd, R. S. (1995) *J. Biol. Chem. 270*, 19501−19508.
34. McCullough, A. K., Sanchez, A., Dodson, M. L., Maraka, P., Taylor, J.-S., and Lloyd, R. S. (2001) *Biochemistry 40*, 561−568.

BI011524U